EXAFS study of structural characteristics of nanocrystalline selenium with different grain sizes

Y. H. Zhao and K. Lu*

State Key Laboratory for Rapidly Solidified Non-equilibrium Alloys, Institute of Metal Research, Chinese Academy of Sciences, Shenyang 110015, People's Republic of China

T. Liu

Synchrotron Radiation Laboratory, Institute of High Energy Physics, Chinese Academy of Sciences, Beijing 100039, People's Republic of China

(Received 8 September 1998)

Extended x-ray-absorption fine-structure measurements (EXAFS) were performed on nanocrystalline (nc) elemental Se samples with grain sizes ranging from 13 to 60 nm. Accompanied with the previous study, we concluded that, with the refinement in nc Se, the intrachain structure (the bond length, the coordination number) is unchanged while the interchain spacing is enlarged. The grain boundary in the nc Se is found to be in a low-energy configuration that is different from the disordered ''gaslike'' grain boundary structure. [S0163-1829(99)01014-0]

Microstructure characteristics of nanocrystalline (nc) materials have been intensively investigated in recent years. Meanwhile, controversial results were obtained in characterizing the grain boundary (GB) structure, that constitutes a large volume fraction in the nc materials,[1–4] the lattice structure of nm-sized crystallites in several nc samples has been found to deviate from that of the perfect single crystal.[5,6] Such a lattice structure distortion, besides the large amount of nonequilibrium GB's, may play a vital role in property variation of nc materials with respect to their conventional coarse-grained polycrystalline counterparts.

In our previous papers,[6,7] quantitative x-ray-diffraction (XRD) measurements reveal an evident variation of the lattice structure parameters (lattice parameter, Debye-Waller parameter, and Debye temperature) and thermal expansion coefficient with the grain size in nc element Se samples. These experimental observations provide strong evidence that even in nc elements the lattice structure of nm-sized crystallites may be distorted and deviated from that of the equilibrium perfect lattice. It is known that trigonal selenium consists of helical $[\text{Se-}]_n$ chains.[8] Se atoms in the chain are bonded with covalent bond, and the $[\text{Se-}]_n$ chains are bonded with Van der Waals forces (see Fig. 1 of Ref. 9). From the lattice structure parameters determined from XRD measurements, which are averaged from all atoms involved in the Bragg reflection, one cannot distinguish the lattice distortion existing at intra- or interchain. In order to identify the origin of the lattice distortion in nc Se, it is necessary to investigate the grain size dependence of the intra- and interchain structure parameters, such as the bond length, the coordination number, etc.

In this paper, we will report a quantitative extended x-ray-absorption fine-structure (EXAFS) investigation on the porosity-free nc element selenium samples (that were used in our previous work[6,7]) with different grain sizes ranging from 13–60 nm.

The nc Se specimens were synthesized by completely crystallizing the melt-quenched amorphous Se (a-Se) solid, of which the procedure was described in detail in Ref. 6,

Table I lists the annealing conditions and the mean grain sizes of the nc-Se specimens used in the present work. For comparison, an as-quenched a-Se sample was also studied.

EXAFS measurements were carried out at the beamline 4W1B (with an energy range of 3.5~22 keV) of Beijing Synchrotron Radiation Facility for High-Energy Physics. The storage ring current was 50–80 mA at 2.2 GeV, and the EXAFS spectra were measured at room temperature. The absorption coefficient at Se K edge was determined using a Si(111) double crystal monochromator and ion-chamber detectors. In order to minimize the absorption of high-energy x-ray harmonics, the monochromator was detuned about 30% and the ion chamber monitoring the incident beam was filled with argon gas and that monitoring the transmitted x ray filled with a mixture of argon (75% vol.) and nitrogen (25% vol.). Powder samples suitable for EXAFS measurements (particle size less than 400 mesh) were ground from the bulk nc-Se and a-Se samples, taking care of the severe requirements of thickness and homogeneity for accurate absorption measurements.

Figure 1 shows the measured x-ray-absorption spectra of a-Se and different nc-Se samples, from which no distinct difference among the spectra of the samples was found.

Since the oscillatory part of the x-ray-absorption contains the structural information, we isolate the fine structure and invert it to obtain the structural parameters in the following way (details of the procedure are given in Refs. 10 and 11). The curve, $a_1 E^{-3} + a_2 E^{-4} + a_3$ (with photon energy E, parameters a_1, a_2, and a_3), was fitted to the data in the pre-

TABLE I. A list of the annealing temperature and the resultant mean grain size in the as-crystallized nc-Se samples. The mean grain size was derived from XRD experiments and verified by TEM observations.

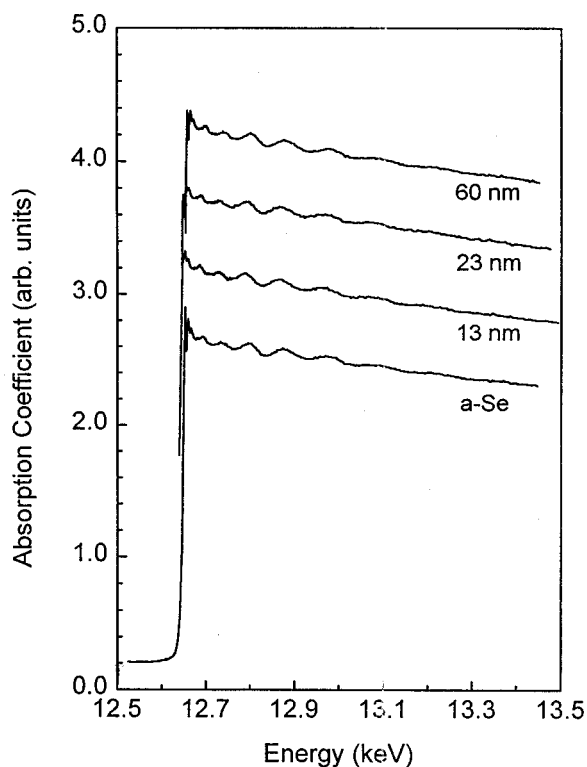| Sample	A	B	C	D
Annealing temperature (K)	--	363	403	470
Mean grain size, D (nm)	a-Se	13±2	23±2	60±6

FIG. 1. X-ray-absorption spectra of a-Se (A) and nc-Se samples with different grain sizes ($B = 13$ nm, $C = 23$ nm, and $D = 60$ nm).

edge region of Se K-absorption edge and another least-square spline is fitted in the post-edge region. The EXAFS χ can be derived by removing the least-square spline from the data and normalizing by $t(CE^{-3} - DE^{-4})$ where t is the thickness parameter and parameters C,D were given in Ref. 12. The derived EXAFS are then converted as a function of the photoelectron wave number k ($= [2m(E - E_0)/\hbar^2]^{1/2}$ where E_0 was chosen at the top of the first peak in the absorption spectra of all samples, and m the electron mass). Figure 2 shows the EXAFS $k^2\chi(k)$ of a-Se and nc-Se samples as a function of k. It can be seen that a-Se and nc-Se samples possess very similar EXAFS oscillations.
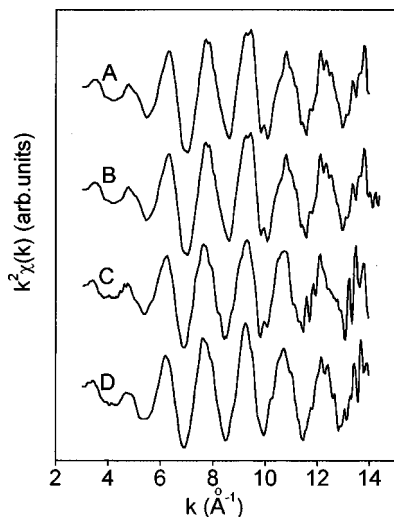

FIG. 2. EXAFS $k^2\chi(k)$ data for a-Se and nc-Se samples after background removal and normalization.
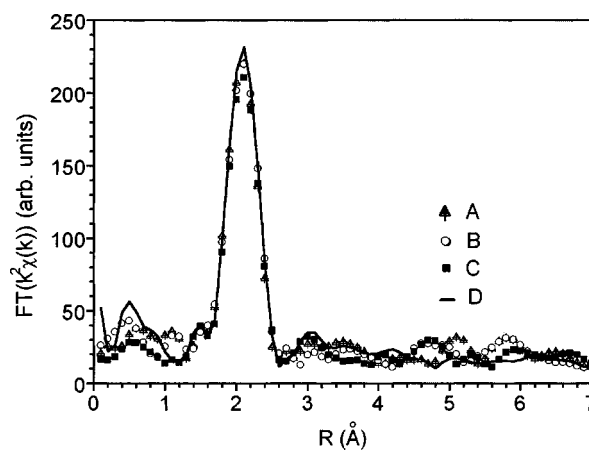

FIG. 3. The magnitude of Fourier transform for a-Se and nc-Se samples. The transform range was from 3.0–14.0 Å, and the data were weighted by k^2 before the transform.

The next step in the analysis is to Fourier transform[10,11] $k^2\chi(k)$ using the region from 3.0–14.0 Å^{-1}. This converts the data from a representation in terms of k to that in terms of coordinate space R and gives an overview of the average radial distribution in the material. Typical results of Fourier transform $FT(\chi k^2)$ for a-Se and nc-Se samples are shown in Fig. 3. It is clear that the EXAFS from all samples contain only a first-shell signal, and the prominent peaks due to the first-nearest selenium atoms are observed at $\sim$2 Å. The second- and third-nearest peaks are not found for a-Se and nc-Se samples for large structural defects. Moreover, it can be seen that the amplitudes of the first shell of $FT(\chi k^2)$ for samples B (13 nm) and C (23 nm) are only about 6 and 8% smaller than that for D (60 nm). These reductions are much smaller than those for nc Pd (21%, 16 nm), Cu (32%, 10 nm), and W (52%, 5–15 nm).[2] From Fig. 3, one can also see that the amplitude of the first peak of $FT(\chi k^2)$ for a-Se is smaller than those for nc-Se samples. This is in agreement with other amorphous semiconductors (such as a-Si,[13] a-Ge[14]) of which the nearest-neighbor peak slightly decreases with going from the crystalline to the amorphous state as a result of structural disorder.

In order to obtain the structural parameters of the first shell, the Fourier-transformed data were filtered and back-Fourier transformed into k space, then fitted by the least-square curve based on a single scattering theory.[15] The fitting results were listed in Table II. The coordination number, co-ordination distance (bond length), and the Debye-Waller factor are found to be nearly unchanged within the measurement error for a-Se and different nc-Se samples. These values are in agreement with the data reported in Refs. 16–18. For the a-Se film, the coordination number is 2.15 and the bond length is 2.32 ± 0.01 Å. For the crystalline films of Se, the bond length is 2.36 ± 0.01 Å.[16] The Debye-Waller factor in the present study are different from those from the XRD measurements for nc Se samples which were found to increase from 0.034 (60 nm) to 0.044 Å^2 (13 nm).[6] The difference may result from the different analysis methods: EXAFS gives the Debye-Waller factor of the first-shell atoms, while the XRD obtains it averaged from all atoms involved in the Bragg reflection.

TABLE II. The structure parameters for a-Se and nc-Se samples by the least-squares curve fitting of the filtered $FT(\chi k^2)$ data based on a single scattering theory (Ref. 15).

Sample	Coordination number (Se-Se)	Bond length (Å)	Debye-Waller factor (Å^2)
A	2.14±0.03	2.35±0.02	0.016±0.001
B	2.15±0.03	2.36±0.02	0.016±0.001
C	2.05±0.03	2.37±0.02	0.018±0.001
D	2.14±0.03	2.36±0.02	0.016±0.001
E[a]	2.15±0.03	2.32±0.02	--

[a]The values for a-Se film from Ref. 16.

According to Ref. 8, the bond length of nc Se, l, can be obtained from measured lattice parameters (a and c, the calculation of a and c was described in detail in Ref. 6):

$$l^2 = (\tfrac{1}{3} c)^2 + (ma)^2 \tag{1}$$

with $l_0 = 2.373$ Å, $a_0 = 4.3662$ Å, and $c_0 = 4.9536$ Å ($m = 0.3903$). Figure 4 shows the bond lengths of nc Se from XRD and EXAFS measurements. It can be seen that the bond length keeps a constant value within the measured error ($\pm 1\%$) against the grain size, and the results from XRD agree well with those from the EXAFS measurements. The grain size independent of the bond length in nc Se suggests that the atomic intrachain structure is unchanged compared to that in the equilibrium perfect lattice.

XRD results revealed that the lattice parameter a increases significantly with a reduction of grain size in nc Se, implying that the interchain spacing is enlarged. This phenomenon can be qualitatively understood by the fact that the covalent bonds intrachain are much stronger than the Van der Waals force interchain. Or in other words, when the nc-Se grain size becomes smaller, i.e., more GB's are created, the interaction between GB's with the nm crystallite results in a distortion in the crystallites (near the GB's region). This distortion may exhibit anisotropy that the interchain arrangement (which are bonded by relative weaker Van der Waals forces) may be preferably altered compared with that intrachain (which are dominated by strong covalent bonds). As a result of minimization of the total energy of crystallite and GB, the interchain spacing is dilated while the covalent bond length keeps unchanged. More accurate data of the parameters are needed to identify the detailed intrachain structure (such as the bonding angle).

Previous EXAFS studies[2] on nc Cu, Pd (fcc), and W (bcc) by consolidation from ultrafine particles observed a large intensity reduction in first shell of the Fourier transform compared to those of the coarse-grained polycrystalline counterparts. The mean coordination numbers were found to decrease from 12 (for coarse-grained Cu, Pd) to about 10.5 (nc Cu), and 10.9 (nc Pd). These results were interpreted in terms of a ''gaslike'' GB structure that differs structurally from either the crystalline or the glassy state in the GB component. However, in present work, when the mean grain size decreases from 60–13 nm, the Fourier transform amplitude was only reduced by a few percent and the coordination numbers were unchanged. The relative small reduction of Fourier transform intensity with decreasing grain size of hcp nc Se agrees with the observation in the XRD measurements.[6] The background intensity from XRD patterns of 13-nm Se was found to decrease by about $11\pm 7\%$ compared to that of 70-nm Se, this reduction is much smaller than that of nc Fe.[1] The GB enthalpy in nc Se was measured experimentally.[19] It was found that the GB enthalpy is comparable to the small-angle GB energy, and it decreases (rather than increases) with a reduction of grain size. These observations imply that the GB structure in the present nc Se is in a low energy configuration, that is substantially different from that of the disordered gaslike GB. More recently, De Panfilis $et\ al.$[20] reported an EXAFS study of nc-Pd samples subjected to various treatments by considering the distribution of particle sizes, the observed reduction in average coordination number can be explained as a size effect originating from the reduced coordination of the atoms present in the surface of the particles, and no further reduction was found, which is in contrast to Ref. 2. Eastman also observed the similar results.[21] Moreover, to avoid the experimental artifacts which erroneously lower the apparent coordination number in transmission mode, Stern[22] measured the nc Cu (13 nm) by the total electron yield technique and found that the GB structure, on the average, is similar to that in conventional polycrystalline Cu, contrary to previous EXAFS measurements made in transmission which indicated a lower coordination number. Further experiments (such as high-resolution electron microscopy) are needed to identify the nature of GB structure of nc Se.

In summary, according to the EXAFS measurements of nc-Se samples and previous study, we found that, with a reduction of grain size, the intrachain structure of nc Se are unchanged while the interchain spacing is enlarged. The gaslike grain boundary structure has not been detected in the nc Se samples.
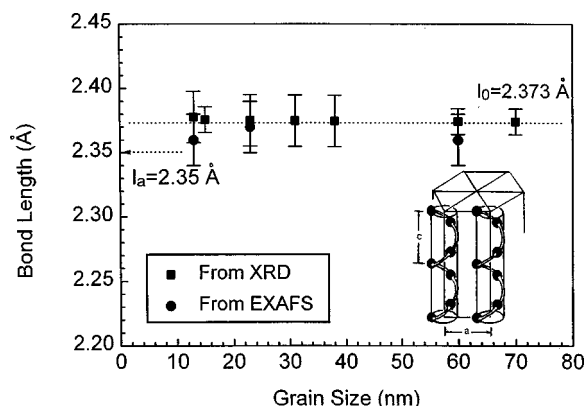

FIG. 4. The bond length of nc Se from EXAFS and XRD measurements against the mean grain size, and the schematic representation of the trigonal Se structure (Ref. 9).

*Corresponding author. Fax: +86-24-2389 1320; electronic address: kelu@imr.ac.cn

[1] X. Zhu, R. Birringer, U. Herr, and H. Gleiter, Phys. Rev. B **35**, 9085 (1987).

[2] T. Haubold, R. Birringer, B. Lengeler, and M. Gleiter, J. Less-Common Met. **145**, 557 (1988); T. Haubold, W. Krauss, and H. Gleiter, Philos. Mag. Lett. **63**, 245 (1991).

[3] G. J. Thomas, R. W. Siegel, and J. A. Eastman, Scr. Metall. Mater. **24**, 201 (1990).

[4] M. R. Fitzsimmons, J. A. Eastman, M. Müller-Stach, and G. Waller, Phys. Rev. B **44**, 2452 (1991).

[5] K. Lu and M. L. Sui, J. Mater. Sci. Technol. **9**, 419 (1993); M. L. Sui and K. Lu, Mater. Sci. Eng. A **179/180**, 541 (1994); K. Lu, Mater. Sci. Eng. R **16**, 161 (1996).

[6] Y. H. Zhao, K. Zhang, and K. Lu, Phys. Rev. B **56**, 14 322 (1997).

[7] Y. H. Zhao and K. Lu, Phys. Rev. B **56**, 14 330 (1997).

[8] P. Ungar and P. Cherin, in *The Physics of Selenium and Tellurium*, edited by W. C. Cooper (Pergamon, Oxford, England, 1969), p. 223.

[9] H. M. Isomäki and J. von Boehm, Phys. Rev. B **35**, 8019 (1987).

[10] E. A. Stern, D. E. Sayers, and F. W. Lytle, Phys. Rev. B **11**, 4836 (1975).

[11] E. A. Stern and S. M. Heald, in *Handbook of Synchrotron Radiation*, edited by E. E. Koch (North-Holland, Amsterdam, 1983), Chap. 10, Vol. 1B.

[12] C. H. Macgillavry, G. D. Riech, and K. Lonsdale, *Int. Tables for X-ray Crystallography* (The Kynoch Press, England, 1972), Vol. 3, p. 161.

[13] M. Wakagi, K. Ogata, and A. Nakano, Phys. Rev. B **50**, 10 666 (1994).

[14] M. Wakagi, M. Chigasaki, and M. Nomura, J. Phys. Soc. Jpn. **56**, 1765 (1987).

[15] E. A. Stern, Phys. Rev. B **10**, 3027 (1974).

[16] A. V. Kolobov, H. Oyanagi, K. Tanaka, and Ke. Tanaka, Phys. Rev. B **55**, 726 (1997).

[17] N. F. Mott and E. A. Davis, *Electronic Processes in Non-Crystalline Materials*, 2nd ed. (Clarendon, Oxford, 1979), p. 581, and references therein.

[18] D. Hohl and R. O. Jones, Phys. Rev. B **43**, 3856 (1991).

[19] K. Lu and N. X. Sun, Philos. Mag. Lett. **75**, 389 (1997).

[20] S. De Panfilis, F. D'Acapito, V. Haas, H. Konrad, J. Weissmüller, and F. Boscherini, Mater. Sci. Forum **195**, 67 (1995).

[21] J. A. Eastman, M. R. Fitzsimmons, M. Müller-Stach, G. Waller, and W. T. Elam, Nanostruct. Mater. **1**, 47 (1992).

[22] E. A. Stern, R. W. Siegel, M. Newville, P. G. Sanders, and D. Haskel, Phys. Rev. Lett. **75**, 3874 (1995).